BBAA VI International Colloquium on:
Bluff Bodies Aerodynamics & Applications
Milano, Italy, July, 20-24 2008

ANALYSIS OF THE NON-STATIONARY FLOW AROUND A RECTANGULAR CYLINDER

Stefano Malavasi*, Marco Negri†

* Dept. of I.I.A.R.
Politecnico di Milano, piazza Leonardo da Vinci 32, 20133 Milano, Italy
e-mail: Stefano.Malavasi@polimi.it,

† Dept. of I.I.A.R.
Politecnico di Milano, piazza Leonardo da Vinci 32, 20133 Milano, Italy
e-mail: Marco3.Negri@mail.polimi.it,

Keywords: rectangular cylinder, PIV, confined flow, topological flow structure, vortex trail.

Abstract. *The non-stationary flow structure around a rectangular cylinder immersed in a water steady flow is analyzed through topological analysis of time resolved PIV velocity fields. The phenomenon considered is characterized by the presence of large scale eddies, which are the main responsible of the hydrodynamic loading on the cylinder. In order to investigate the correlation between the hydrodynamic loading and the flow structures, we have identified and measured the motion of large scale eddies generated by the flow separations through the tracking of their vortex centres. The leading and trailing vortices have been characterized by calculating their convection velocity and shedding frequency.*

1 INTRODUCTION

In this paper we studied the non-stationary flow around a rectangular cylinder through the topological analysis of time resolved PIV velocity fields. We focused our investigation on the characterization of the motion of large scale eddies generated by the flow separations. The aim of this study is to increase the knowledge on the relationship between hydrodynamic loading and flow structures.

Even if it is one of the simplest geometry, rectangular cylinder has reference to various engineering applications, like civil works as bridges and skyscrapers. When an elongated rectangular cylinder is immersed in a flowing flow, generally a flow separation occurs at the leading and trailing edges, and large scale vortices are shed; flow reattachment in the lateral regions may appear or not in relation to the elongation of the of cylinder the flow characteristics and to the boundary conditions. The structure of the flow is considered the main responsible of dynamic loading on the obstacle hence the dynamic state of the obstacle could be better understood by the characterization of the evolution of the coherent structures generated around the cylinder. Literary studies on this topic have followed out especially the case of unbounded or symmetrical bounded flow; in this configuration the motion of the large fluid structures has been quite investigated. Precise values of convection velocity and shedding frequency have been measured or calculated by several researchers in the different region of the flow around the obstacle. Most of literature studies

on unsteady flow are made with a eulerian approach, *e.g.* correlation or frequency analysis of local measurements of pressure or velocity. With these methods the properties of the flow field are extracted without directly considering the instantaneous location and movements of the vortices, but the time-history of a property of the flow related to them. In this work we have developed an analysis based on a lagrangian approach: the position of vortices is detected at each time "instant" and velocity convection and shedding frequency are calculated from vortex trajectories. The results obtained with this approach are comparable with those of literature in similar fluid-dynamic conditions; moreover the visualization of the flow evolution facilitates the comprehension of the phenomenon.

In recent works Malavasi and Blois [7] showed a good correspondence between some parameters related to the mean flow structure around a rectangular cylinder and the mean coefficient of drag and lift measured by Malavasi and Guadagnini [6] in the same configuration. They investigated the case of a cylinder immersed in free surface flow and found out that both mean flow structures and dynamic solicitation are strongly dependent on the distance from confinement surfaces.

In this work we analyzed the same time-resolved PIV experimental data used by Malavasi and Blois [7] to study the unsteady flow around the rectangular cylinder.
We especially considered two flow conditions: the first one, which mimics a symmetrical mean flow structure and the second one, characterized by flow asymmetry induced by the presence of a solid wall near the cylinder.

2 EXPERIMENTAL CASES

As before mentioned, in this work we used the same time-resolved PIV experimental data used by Malavasi and Blois [7], therefore, a brief description of the experimental set-up is offered. The experimental data considered were acquired in an open channel with a steady free surface flow in which a rectangular cylinder was placed at several elevations above the channel floor. The channel had a rectangular section of 0.5 m width and 0.6 m height and the rectangular cylinder here used had a longitudinal dimension L=0.18 m, a vertical section s=0.06 m (aspect ratio L/s=3) and spanned the whole width of the channel.

The velocity field were obtained using a particular time-resolved PIV technique (Malavasi *et al.* [5]); it consists in capturing long-exposed images of the seeded flow (shutter time was set to 0.02 s) using a CCD camera, so that particles impress their trajectory on each image. Measuring these trajectories it is possible to obtain, through a series of elaboration steps, a velocity field. The acquisition frequency was 50 Hz, and the duration of each acquisition, due to the memory storage capacity, was 32 s. The measure plane was vertical, parallel to the flow and situated in the median section of the channel. The experimental configuration was described essentially by three parameters, related to the thickness s of the cylinder (Fig.1) :

- $Re = \rho U_0 s/\mu$; Reynolds number;
- $h^* = (h_m - h_b)/s$; dimensionless distance of the intrados from the free surface, where h_m is the water depth at the upstream control section and h_b is the elevation of the cylinder from the channel floor
- h_b/s dimensionless elevation of the cylinder;

Fig.(1) represents the case with h_b/s=2.33 and h^*=5, which is the first case considered. Moreover the case with h_b/s=1 and h^*=5 was analyzed. In both cases the Reynolds number was Re=1.2 10^4 and the turbulence level Tu=14 %.

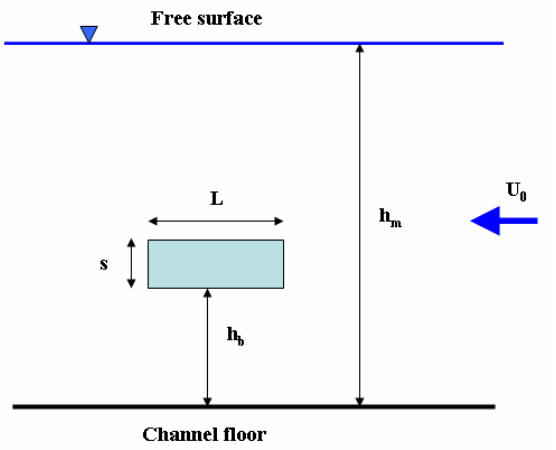

Fig. 1: Experimental configuration.

Malavasi and Blois [7] pointed out that the first case (h_b/s=2.33 and h^*=5) mimics quite well the unbounded or symmetrical bounded condition. Indeed, as it is shown in Fig.(2), the mean flow field around the structure depicts a quasi-symmetrical structure and moreover the lift coefficient in this situation is rather null (Malavasi and Guadagnini [6]). We chose this case because under these conditions it is possible to compare our results with literature studies which generally report symmetrical bounded flow. The second case (Fig. 3) was chosen to verify how the significant asymmetry that characterizes the mean flow is detectable in the temporal evolution of the flow structures.

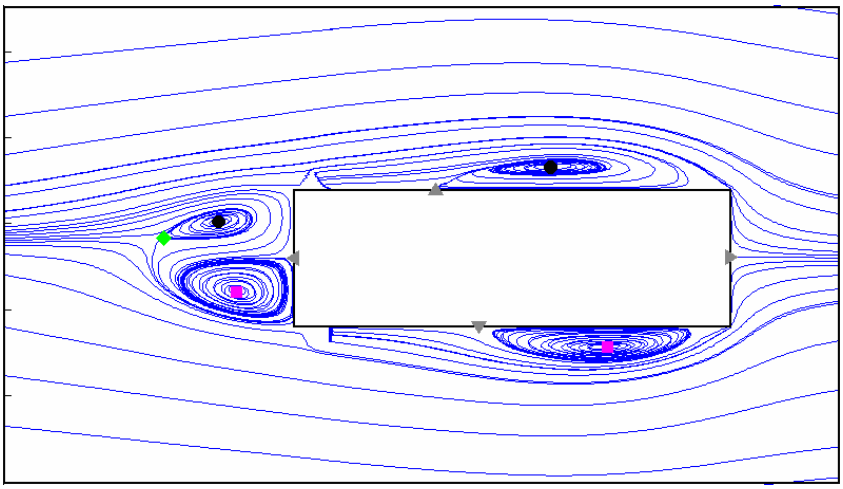

Fig. 2: Mean flow structures (h_b/s=2.33, h^*=5); ●, anticlockwise vortex; ■, clockwise vortex; ♦, ▲, saddle points.

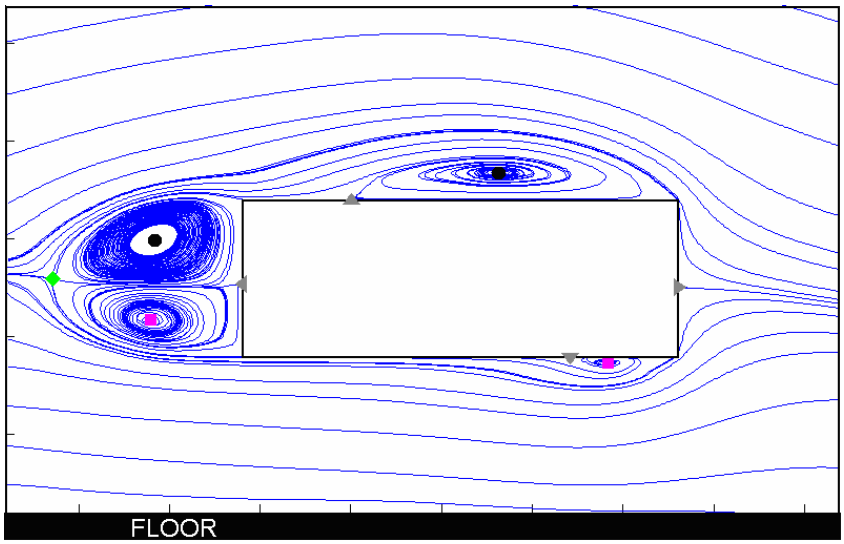

Fig. 3: Mean flow structure (h_b/s=1, h^*=5); ●, anticlockwise vortex; ■, clockwise vortex; ♦, ▲, saddle points.

3 ANALYSIS TECHNIQUE

As before introduced, the analysis here proposed is focused on the characterization of the motion of the main vortex structures involved in the vortex shedding phenomenon. This analysis was carried out by means of Velocity Inversion Points (VIP) technique which was used in a previous work by Malavasi and Blois [7] for the reconstruction of the mean flow structure of flow around the same obstacle. Starting by these previous results, we improved vortex detecting algorithms and set a series of filters and tracking algorithms which allowed the characterization of the shedding of the main vortices through tracing the path of their vortex centers.

VIP technique basis on the localization of the inversion points of two components of the velocity inside the 2D velocity fields. Fig.(4) shows the four kinds of inversion points that can be defined. They are catalogued depending on the component of the velocity (horizontal component u or vertical component v) and the direction along which the inversion is calculated (horizontal direction x or vertical direction y); moreover each kind of these can be positive or negative depending on the inversion sign. The case A and D may be correlated to a rotational component of the flow field, while B and C express linear deformation of the flow fields. Connecting velocity inversion points of certain typologies it is possible to obtain the inversion lines which are able to highlight some features of the flow structures. As reported in Fig.(5) and Fig.(6), Malavasi and Blois [7] showed how the inversion lines characterize the mean vortex structures, for example detecting the reattachment point and the vortex centers.

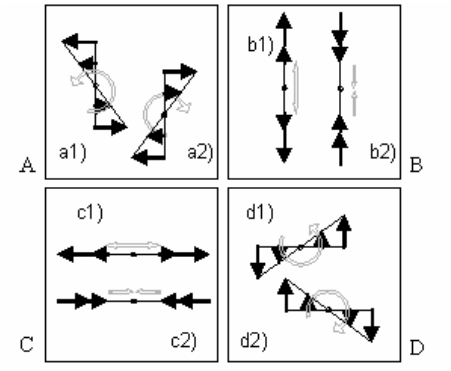

Fig. 4: Velocity inversion typology (Malavasi and Blois [7]).

Fig.(5) details the lateral regions of the cylinder where two inversion lines are highlighted: the formation bubble line FBL, locus where u=0 (points of typology A and C) and the deviation line DL, locus where v=0 (points of typology B and D).

The formation bubble line FBL spans the whole dimension of the formation bubble and along that it is possible to detect the vertex point (VP), which is the maximum vertical point of FBL, and the reattachment point (RP), which allows to define the longitudinal ad transversal dimensions of the formation bubble. At the intersection of the FBL and the DL is placed the centre of the main vortex structure.

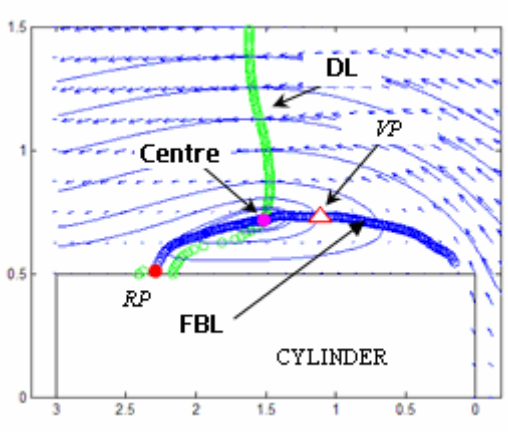

Fig. 5: Flow structures in the extrados (Malavasi and Blois [7]).

In the rear region (Fig. 6) the inversion points allow the identification of the contra-rotating vortex centers and of the formation region (region where the flow direction is opposite to the mean flow). The formation region stands between the formation line (locus where u=0, A and C points) and the obstacle rear surface, while the vortex centers are localized at the interceptions of the formation line with the conjunction lines (CLs, v=0). The mean flow structure in the rear region is moreover characterized by the presence of a saddle downstream the contra-rotating vortices and a half-saddle close to the rear face of the cylinder. All these critical points have a common feature, which is velocity null in the measurement plane. To recognize a vortex center we verify the presence of rotational inversion points of both components of velocity (horizontal and vertical), with the same rotation. For example an anticlockwise vortex centre is detectable if, among the rotational inversion points, only points of typology a1 and d1 are present. The main problem for the developing of unsteady analysis is connected to the quality of the velocity fields and to the setting

of the temporal parameters of the procedure, which depends also to the temporal evolution of the phenomenon.

The original sampling frequency of PIV acquisitions was 50 Hz, and shutter time 0.02 s. A single velocity field is difficult to be directly analyzed, because of the presence of errors or data lack regions. To improve the quality of the "instantaneous" velocity field available by the PIV acquisition, we used a temporal moving average. To catch the real evolution of the flow field, the window width has to be properly set depending on frequency and convection velocity of the vortex structures moving in the flow field; hence a preliminary research on literature studies about vortex shedding around cylinders was useful to provide a first value of the averaging window width. Subsequent tests completed varying the window width allowed to find the best result using a window of width 0.2 s. Considering that the original data were acquired with a 50 Hz sample frequency, adopting a temporal window of 0.2 s means that every time-averaged field is obtained by averaging 10 original velocity fields.

A window width of $1/(25\text{-}50\ U_0)$ s (where U_0 is the undisturbed flow velocity) generally represents a good value to study the phenomenon of vortex shedding.

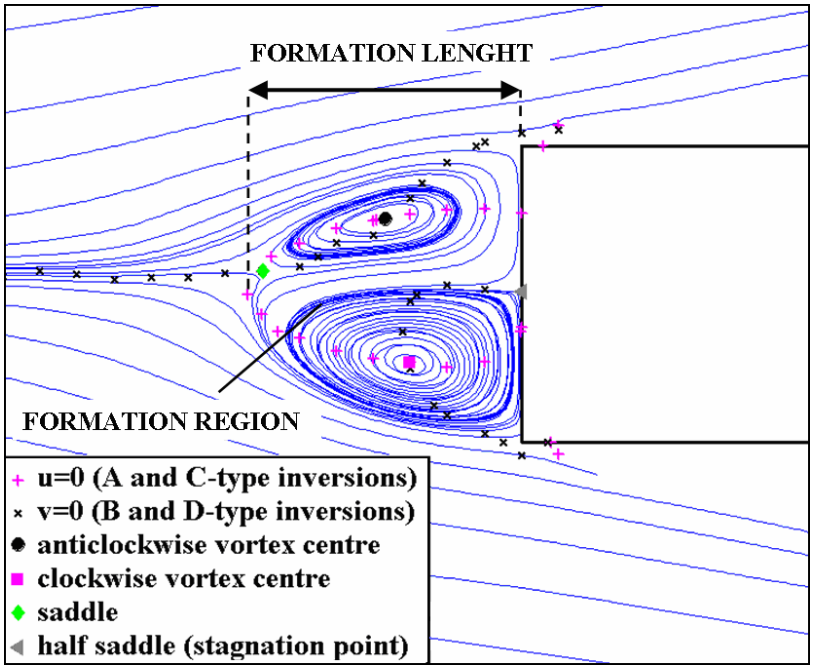

Fig. 6: Mean flow structures in the rear region;

Fig.(7) shows the application of the moving average on a sequence of PIV data. The flow at the extrados clearly evidences the evolution of the vortex structures which are moving towards the trailing edge. On the same figure the vortex center positions, calculated by the application of VIP procedure, are highlighted.

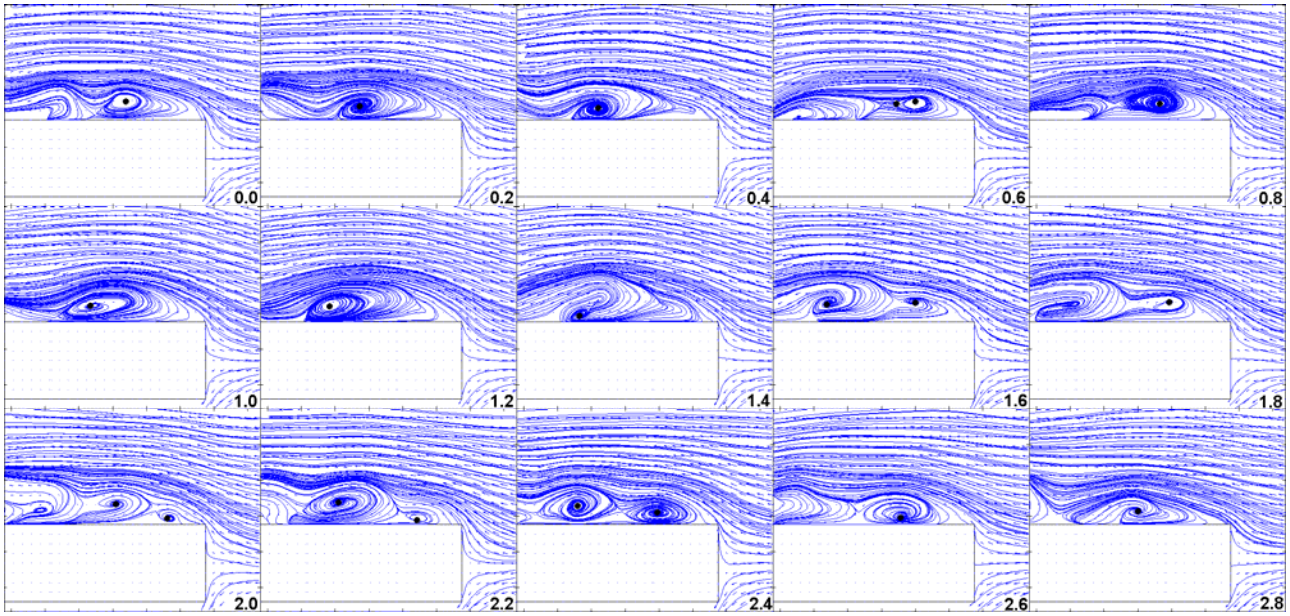

Fig. 7: Flow evolution in the extrados region, h_b/s=2.33, h*=5, Re=1.2• 10^4 (progressive time in seconds).

The vortex center localization is only the first step of the vortex trail reconstruction. As a matter of fact, the presence of erroneous solutions and of more vortices in the same image, increase the difficulties in the temporal vortex trail reconstruction. Fig.(8) shows the position of the vortices center shedding at the extrados versus time. The vortex centre trajectory reconstruction was provided developing a tracking algorithm. The "correspondence problem" (*i.e.* determining the correspondence between features in successive time steps) was solved by considering the possible movements (based on undisturbed flow velocity) of a vortex centre between two consecutive instant of time.

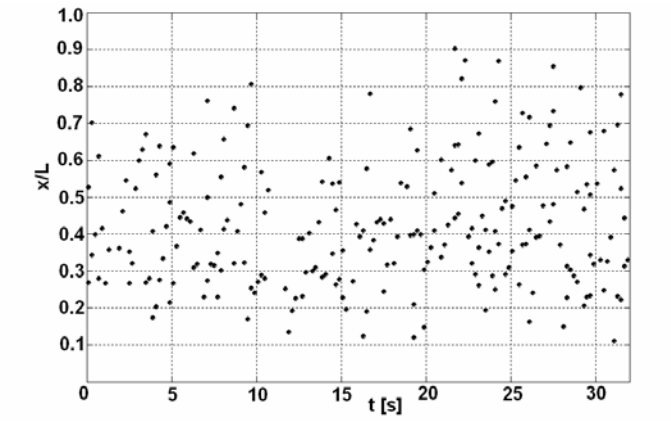

Fig. 8: Position of vortex centers along the rectangular cylinder versus time

Fig.(9) reports movements of the vortex centers along the longitudinal dimension of the obstacle; every line represents the horizontal trail of a vortex from the leading edge toward the trailing edge. The convection velocity of each vortex, therefore, has been calculated as ratio between displacement of the vortex centre and time (Fig. 9). Mean convention velocity of vortices has been obtained averaging the values of the convection velocities of the all reliable trajectories detected. The reliable trajectories were selected applying a filter based on the number of points and

the length of each trajectory. Only trajectory with a minimum length (l_{min}≥0.15 x_R) and a minimum number of points (n_{min}≥3) was used to calculate mean convection velocity; indeed trajectory with few points are more affect by errors due to the temporal averaging of the flow fields, while short trajectory are not as well representative of vortex motion as long ones. These two filtering parameters have to be set in relation to mean length of vortex paths and duration of time step of averaging.

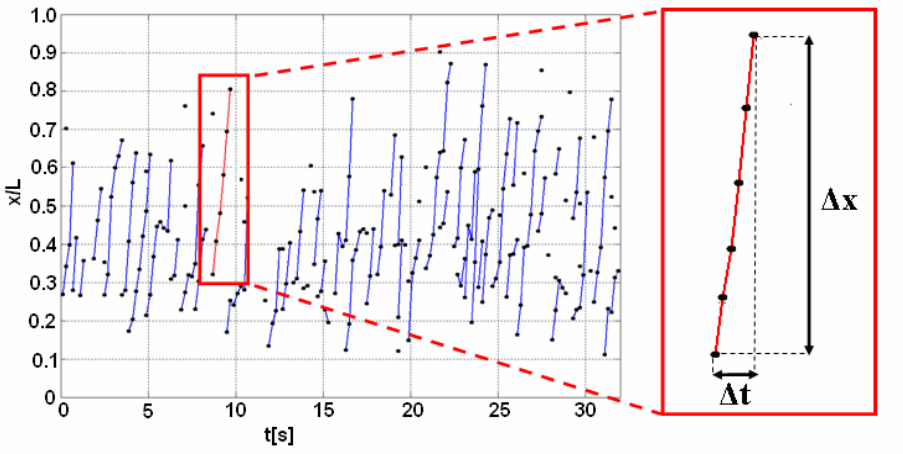

Fig. 9: Vortex center position related to time in the extrados region and calculation of convection velocity along a single trajectory, $u_C=\Delta x/\Delta t$.

Shedding frequency of a vortex has been calculated by counting vortices trajectories that are included or pass through a control region. Ratio between the number of counted trajectory and time is the frequency of vortex crossing through the fixed area. In order to minimize mistakes due to discontinue trajectories, the setting of the control region is crucial for the accuracy of the results.

In the lateral regions we found that the control region defined by the lines is x=0.35 x_R and x=0.6 x_R, where x_R is the mean reattachment point, is a good solution to minimize the error in the procedure. In this way we were able to count almost all vortices that shed from the formation bubble (Fig. 10).

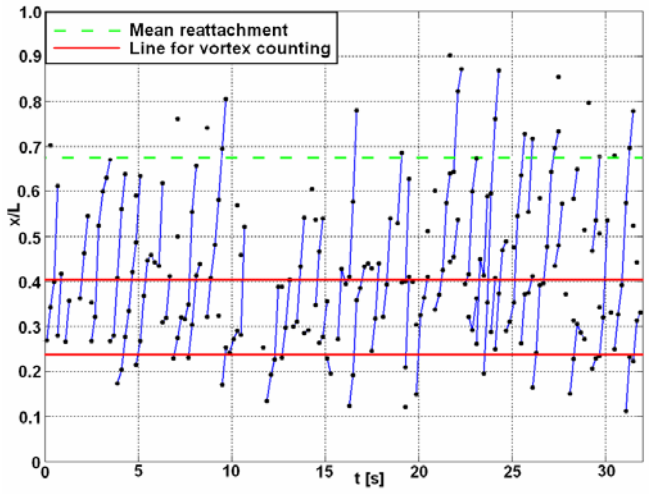

Fig. 10: Vortex center movements related to time. Lines for the calculation of the shedding frequency are reported.

The procedure here discussed was also applied for the detection of the vortices trail in the rear region. In this case clockwise and anti-clockwise vortices were detected; the control region in this case was defined by the lines x=0.2 L_f and x=0.5 L_f, where L_f is the mean longitudinal length of the formation region (L_f/s=1.00 for the case with h_b/s=2.33, L_f/s=1.31 for the case with h_b/s=1).

4 RESULTS

As before discussed, first we considered the condition with h_b/s=2.33. This condition appears to be similar to the unbounded flow one, both for the mean flow configuration, which is quite symmetric, and for the value of the mean coefficients of lift C_L=0 (Malavasi and Blois [7]). Our results refer to 5 PIV acquisitions (one acquisition last 32 s) for each region of the flow field (extrados, intrados, and rear region).

The topological analysis of the mean flow structure (Fig. 2) shows that in the lateral regions the position of the reattachment points, both superior and inferior, is quite backward (2.01 *s* in the extrados and 1.74 s in the intrados) respecting on literature value. This fact is attributable both to the influence of the flow confinement and both to the high level of turbulence; indeed the reattachment length of 2.45 *s* provided by Saathoff and Melbourne [8] corresponds to a flow with Re=4 · 10^5 and Tu=8.2 % while generally, in flow with low turbulent level the reattachment length could reach values of about 4.9-5.0 *s* for elongated cylinder (Cherry *et al.*[1], Kiya and Sasaki [4]).

As mentioned above, for the analysis of the flow structure evolution, we used a non-overlapping averaging time-window of 0.2 s. This value is a good compromise between the need to obtain regular fields (enlarging the temporal window) and to proper represent the instantaneous flow field (tightening the temporal window), therefore to proper caught the frequencies and velocities involved in the phenomenon.

Fig.(7) shows a sequence of flow evolution in the extrados region; anti-clockwise vortices continuously form near the leading edge and move downstream with a quasi horizontal convection velocity. In this case, the calculated velocity of the vortices is u_C=0.41 U_0 (where U_0 is the undisturbed upstream mean velocity) and the vortex frequency is f=1.26 Hz.

Intrados flow field evolution is similar to the extrados one: clockwise vortices periodically forms and proceed downstream. We calculated a mean convection velocity u_C=0.43 U_0 and a vortex frequency f=1.40 Hz.

The different values of reattachment length and shedding frequency underline the light asymmetry between the lateral regions; however if we consider the dimensionless values of frequency of the two regions, they are very similar (Tab.1).

	Kiya-Sasaki 1983	Cherry et al. 1984	Saathoff-Melbourne 1997	Tafti-Vanka (numeric) 1991	Present study	
					extrados	intrados
u_C/U_0	**0.5**	**0.5**	**0.43**	**0.46**	**0.41**	**0.43**
$f \cdot x_R/U_0$	**0.6**	**0.7**	**0.55**	**0.69**	**0.76**	**0.73**
x_R/s	**5.05**	**4.9**	**2.45**	**6.5**	**2.01**	**1.74**
Tu (σ_u/u)	0.2 %	0.07 %	8.2 %	0	14 %	
γ_b	5 %	3.79 %	5.4 %	0	13.6 %	
Re	$2.6 \cdot 10^4$	$3.2 \cdot 10^4$	$4.0 \cdot 10^4$	$1.0 \cdot 10^3$	$1.2 \cdot 10^4$	

Tab. 1: Summary of literature and present values of unsteady flow properties.

As we can see in Tab.(1), where some literature studies in different flow conditions are reported, convection velocity magnitude is included in the range 0.43÷0.5 U_0, while frequency is included in the range 0.55-0.7 U_0/x_R. Present results are very close to these ranges of values. Still frequencies values are a little higher than literature ones, while convection velocities are little smaller; this could be related to the different conditions of our experiments, in which a high level of turbulence, high blockage and asymmetrical confinement are present. Higher frequencies could be due to higher blockage value of our case. An interesting evidence of our investigation is that the vortex centers sometimes make little upstream displacement (Fig. 9); this fact could be the explanation of the slightly low value of convection velocity we calculated.

The mean configuration of the wake in the rear region downstream the cylinder is quite symmetric to the centerline (Fig. 2). It is formed by two contra rotating vortices separated by two saddle points, one on the obstacle surface and one downstream the vortex centers.

It is well known that the predominant mechanism of this region, for a cylinder with this aspect ratio, is the alternate formation and shedding of clockwise and anti-clockwise vortex (TEVS). They form near the obstacle surface and move downstream growing in dimension. This behaviour is depicted in Fig.(11), where one cycle of TEVS mechanism is completed in the first 1.8 s. Besides, in Fig.(11) trajectory of vortex centres are overlapped; in Fig.(12) and Fig.(13) the dimensionless horizontal (x/s) and vertical (y/s) component of these trajectories are provided for the entire time of one acquisition sequence (32 s).

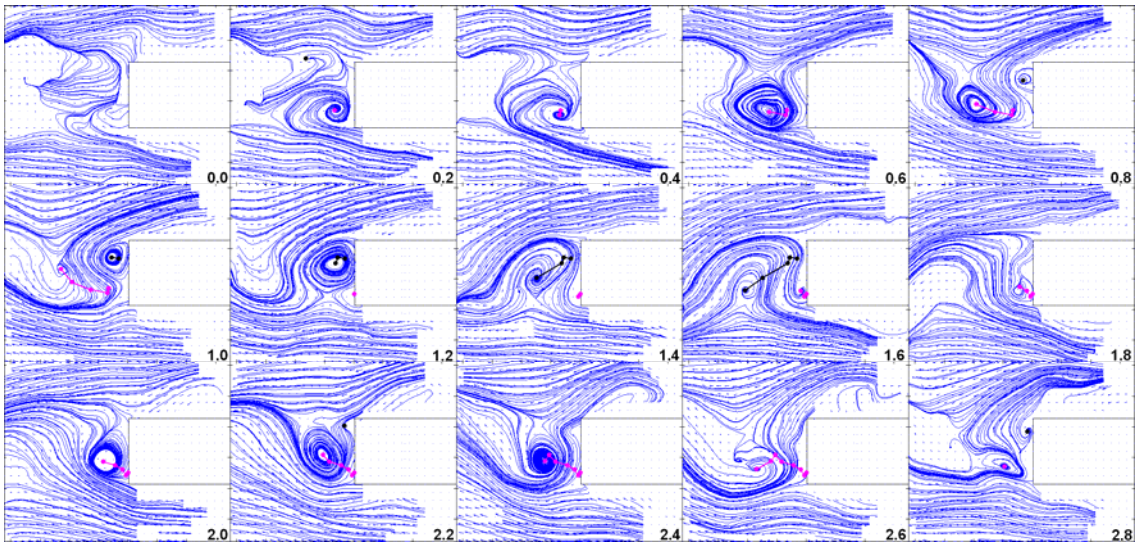

Fig. 11: Flow evolution of base region (progressive time in seconds)

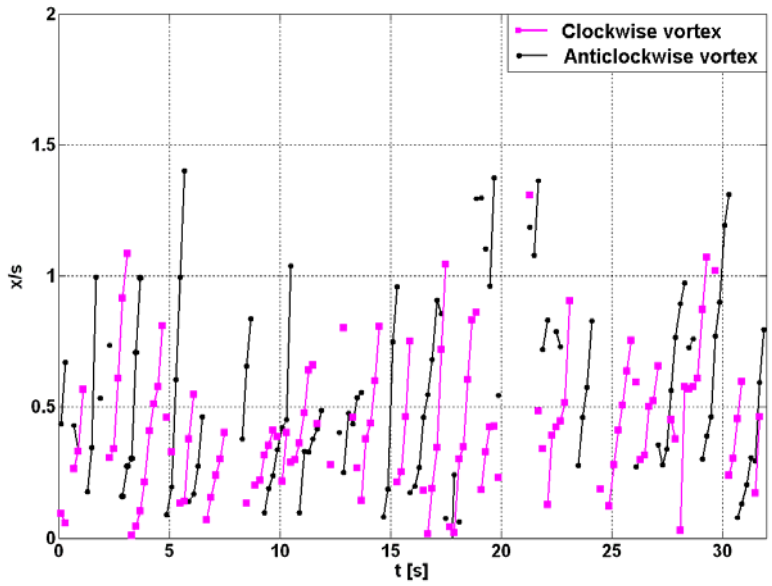

Fig. 12: X movements of the vortex centres versus time.

Mean convection velocities of wake vortices in the base region are 0.27 U_0 for the anti-clockwise vortices and 0.24 U_0 for the clockwise ones. These values are characterized by a high dispersion because of two major aspects: 1) the convection velocity value is affected by a real dispersion; 2) the vortices tend to accelerate in the direction of the flow moving downstream. These aspects are clearly depicted in Fig.(14), where the distribution of the "instantaneous" convection velocity obtained from the data of 10 anticlockwise vortices and 10 clockwise vortices is reported. We comment that, even if this tendency is clear, the dispersion of the data make difficult to find a reliable relationship between convection velocity and distance from the obstacle.

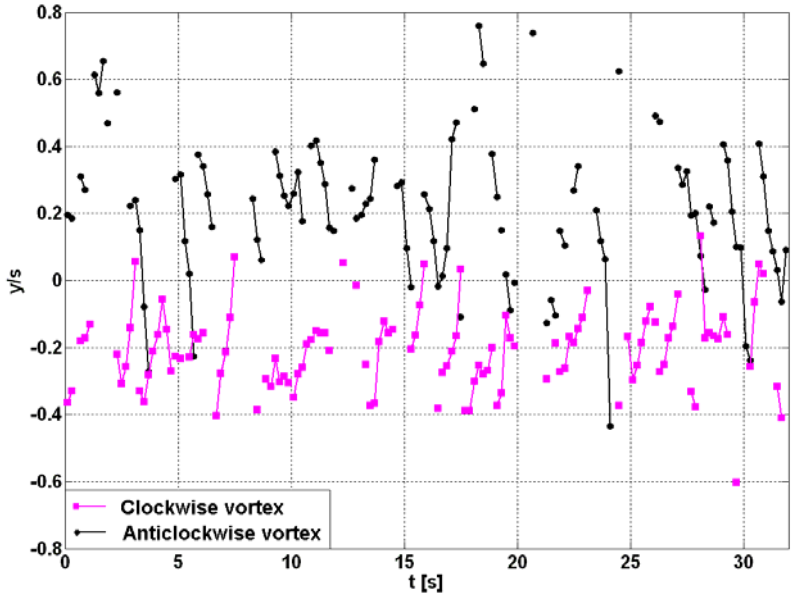

Fig. 13: Y movements of the vortex centres versus time.

In literature, specific studies about vortex movement in the base region of a rectangular cylinder are not found, notwithstanding our results agree with experimental evidence of Nakagawa *et al.* [12] who found, in the near wake of a cylinder with the aspect ratio L/s=3 and a blockage coefficient of 20 %, a convection velocity u_C=1.04 U_0. Moreover, increasing of convention velocity is observed also for different shapes of obstacle: Lyn et al. [2] for a square cylinder found u_C=0.43 U_0 in the region $x/s \leq 3$ and u_C=0.78 U_0 in the region $x/s \geq 4$; Lin et al. [3] for a circular cylinder found that convection velocity increases for $x/D \leq 5$ and keep constant for $x/D \geq 5$ with a magnitude u_C=0.86 U_0;

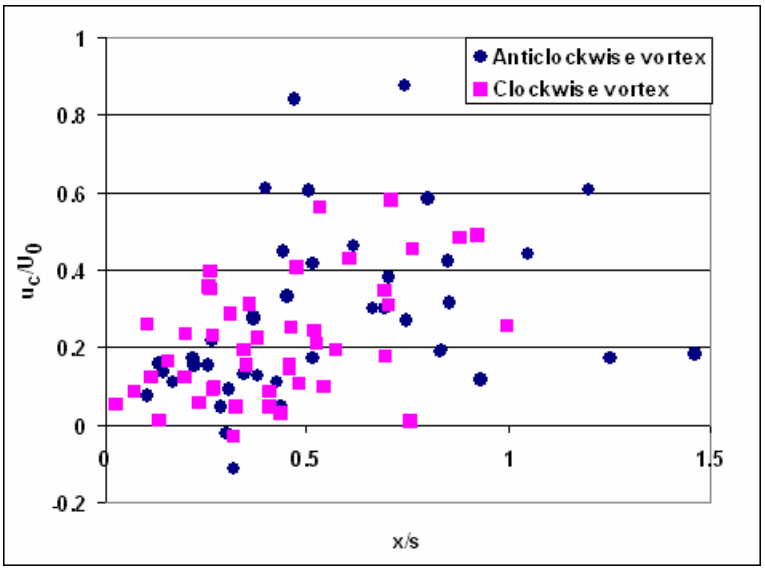

Fig. 14: Local convection velocity versus distance from the obstacle in the base region

As described in section 3, anticlockwise and clockwise vortex frequencies are separately calculated. We obtained a frequency of f=0.63 Hz for anticlockwise vortices and f=0.69 Hz for clockwise vortices. An exact TEVS mechanism involves the same frequency for each kind of vortex, therefore also in term of frequency the slightly asymmetry provided by the boundaries is highlighted. These frequencies or the average one (f=0.66 Hz) are comparable with those of literature. If we considered the Strouhal number associated to the shedding frequency, Okajima [11], for a rectangular cylinder with the same aspect ratio and immersed in an unbounded flow, obtained a Strouhal number St=0.16-0.17.

If we considered our average frequency of 0.66 Hz we obtain a Strouhal number St=0.20. Moreover, if we consider the significant influence of the blockage in our experiment, γ_b=14 %, the corrected Strouhal number becomes St_c=0.18. This latter value was calculated applying the Eq.(1) proposed by Okajima *et al.* [13], in which we used the value n=0.7 as proposed by the same Author for an aspect ratio of L/s=3.

$$St_c = St\,(1-\gamma_b)^n \tag{1}$$

Even if the Eq. (1) was derived for flow solid confinements, Malavasi and Guadagnini [6] showed that is possible to extend its application to free surface confinement, when the obstacle does not distort significantly the free surface of the current (*e.g.* considering high submergence levels). The value of St=0.20 here calculated also confirms the value calculated by Malavasi and

Guadagnini [6] via the analysis of the dynamic loading on the cylinder in a similar configuration. They directly measured drag and lift forces through a dynamometric cylinder.
Besides quantitative information on the main parameter involved in the phenomenon, the analysis here described may give useful qualitative description of the flow structure which helps in the phenomenon interpretation. Fig.(15) depicts the shedding of vortices coming from the extrados which are involved in the wake mechanisms. These vortices, which were sporadically recognised in our analysis, influence the flow structure behind the obstacle and could be probably associable to ILEV mechanism. As it is well known in literature the aspect ratio L/s=3 in very close to the shift of frequency between the two shedding mechanisms.

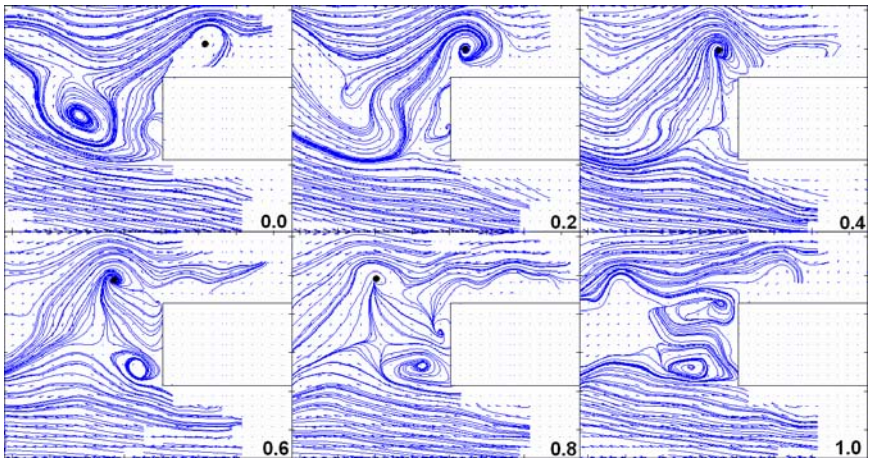

Fig. 15: Convection of a vortex coming from the extrados region

In order to investigate the effects of a solid wall confinement, we also considered the case of cylinder near the channel floor (h_b/s=1, h^*=5 and Re=1.2 · 10^4). As before discussed, the mean flow configuration is quite different changing the cylinder elevation (Fig. 2 and Fig. 3). Fig.(3) highlight how the flow field in the lateral regions is very asymmetric, indeed, the different dimension of the two formation bubbles on the sides of cylinder is evident (x_R/s= 2.25 for the extrados and x_R/s=0.74 for the intrados); this fact is mainly imputable to the floor proximity.

The small dimension of the formation bubble in the intrados precludes the possibility of the unsteady description of the phenomenon with the temporal and spatial resolution available in our PIV data. Notwithstanding, the analysis of the flow at the extrados provides significant experimental evidences. We observed that the mean convection velocity of extrados vortices is not very different from the former case, while significant differences could be observed by comparing the vortex frequency. We calculated f=1.5 Hz, corresponding to 1.01 U_0/x_R, which is a value higher than the values of the symmetrical cases previous discussed.

In the base region, equally the convention velocities are similar for the two case considered (0.24 U_0 for anticlockwise vortices and 0.25 U_0 for clockwise vortices), while the frequency is 0.73 Hz, which correspond to a St=0.22, a little higher than before. This result agrees with Davis *et al.* [10], which demonstrated that the of Strouhal number increases with the blockage.

5 CONCLUSIONS

The non-stationary flow around a rectangular cylinder has been experimentally investigated: two-dimensional velocity fields obtained from PIV acquisitions have been analyzed using a lagrangian approach. Since vortex shedding is the most responsible of dynamic loading on

immersed structures, we traced the movements of vortex centers inside the flow field. To do this, first we applied a moving time-average on the original velocity fields in order to have more regular velocity fields; then we detected the position of the vortex centers at various time instant by means of VIP technique (Malavasi and Blois [7]); with these positions we reconstructed the trajectory of the vortex centers inside the flow field. The whole methodology was computerized.

We were able to characterize the vortex evolution by calculating the mean convection velocity and frequency of the vortex shedding on lateral sides and in the base region of the cylinder. Our results are comparable with literature for the case with quasi symmetrical mean flow condition; moreover they show significant difference for the case of asymmetrical flow configuration (Fig. 2). Besides the quantitative results discussed, the reconstruction of the 2D velocity field evolution offers the possibility of a better understanding of the investigated phenomenon.

REFERENCES

[1] N. J. Cherry, R. Hillier, M. E. P. Latour. Unsteady measurement in a separated and reattaching flow. *Journal of Fluid Mechanics*, **144**, 13-46, 1984.

[2] D. A. Lyn, S. Einav, W. Rodi, J. H. Park. A laser-doppler velocimtry study of confined flow around rectangular cylinders. *Journal of Fluid Mechanics,* **304**, 285-319, 1995.

[3] C. Lin, S. C. Hsieh. Convection velocity of vortex structures in the near wake of a circular cylinder. *Journal of Engineering Mechanics*, **129**, 1108-1118, 2003.

[4] M. Kiya, K. Sasaki. Structure of a turbulent separation bubble. *Journal of Fluid Mechanics,* **137**, 83-113, 1983.

[5] S. Malavasi, S. Franzetti, G. Blois. PIV Investigation of flow around submerged river bridge. Proceedings of the River Flow 2004, Napoli, Italy, June 23-25, 2004.

[6] S. Malavasi, G. Guadagnini. Interactions between a rectangular cylinder and a free-surface flow. *Journal of Fluids and Structures*, **23**, 1137-1148, 2007.

[7] S. Malavasi, G. Blois. Flow structure around a rectangular cylinder near a solid surface. Proceedings of the XVIII Congresso AIMETA, Brescia, Italy, September 11-14, 2007.

[8] P. J. Saathoff, W. H. Melbourne. Effect of free-stream turbulence on surface pressure fluctuations in a separation bubble. *Journal of Fluid Mechanics*, **337**, 1-24, 1997.

[9] D. K. Tafti, S. P. Vanka. A numerical study of flow separation and reattachment on a blunt plate. *Phys. Fluids,* **A 3(7)**, 1749-1759, 1991.

[10] R. W. Davis, E. F. Moore, L. P. Purtell. A numerical-experimental study of confined flow around rectangular cylinders. *Phis. Fluids*, **27(1)**, 1984.

[11] A. Okajima. Strouhal numbers of rectangular cylinders. *Journal of Fluid Mechanics*, **123**, 379-398, 1982.

[12] S. Nakagawa, K. Nitta, M. Senda. An experimental study on unsteady turbulent near wake of a rectangular cylinder in a channel flow. *Experiments in Fluids*, **27**, 284-294, 1999.

[13] A. Okajima, D. Yi, S. Kimura, T. Kiwata. The blockage effects for an oscillating rectangular cylinder at moderate Reynolds number. *Journal of Wind Engineering and Industrial Aerodynamics,* 69–71, 997–1011, 1997.